Int. J. Cancer: **118,** 704–713 (2006)

Protein expression profiling identifies maspin and stathmin as potential biomarkers of adenoid cystic carcinoma of the salivary glands

Dai Nakashima[1], Katsuhiro Uzawa[1,4]*, Atsushi Kasamatsu[1], Hirofumi Koike[1], Yosuke Endo[1], Kengo Saito[1], Susumu Hashitani[2], Tsutomu Numata[3], Masahiro Urade[2] and Hideki Tanzawa[1,4,5]

[1]*Department of Clinical Molecular Biology, Graduate School of Medicine, Chiba University, Chiba, Japan*
[2]*Department of Oral and Maxillofacial Surgery, Hyogo College of Medicine, Hyogo, Japan*
[3]*Division of Otorhinolaryngology, National Hospital Organization Chiba Medical Center, Chiba, Japan*
[4]*Division of Dentistry and Oral-Maxillofacial Surgery, Chiba University Hospital, Chiba, Japan*
[5]*Center of Excellence (COE) Program in 21st Century, Graduate School of Medicine, Chiba University, Chiba, Japan*

Adenoid cystic carcinoma (ACC) is one of the most common malignant tumors of the salivary glands. It tends to grow slowly but is associated with a poor prognosis compared to other malignant salivary gland tumors. To identify specific markers of ACC, we examined protein expression profiling in ACC xenograft and normal salivary glands (NSG) using fluorescent 2-dimensional differential in-gel electrophoresis (2-D-DIGE), an emerging technique for comparative proteomics, that improves the reproducibility and reliability of differential protein expression analysis between the samples. To identify the proteins, matrix-assisted laser desorption/ionization time-of-flight peptide mass fingerprinting was carried out. Using these strategies, we detected 4 upregulated proteins and 5 downregulated proteins in ACC xenograft. Maspin and stathmin were selected for further analyses. Western blotting and immunohistochemical staining showed a higher expression of these proteins in ACC xenograft and clinical ACC tissue compared to NSG. Furthermore, Expression of these proteins was correlated with the histologic grading of ACC ($n = 10$). Therefore, our data indicate that maspin and stathmin may be not only useful biomarkers of ACC but also markers of biologic behavior in this tumor.

Key words: maspin; stathmin; adenoid cystic carcinoma (ACC); fluorescent 2-dimensional differential in-gel electrophoresis (2-D-DIGE); immunohistochemistry

Adenoid cystic carcinoma (ACC) is one of the most common malignancies of the major and minor salivary glands.[1–4] Although ACC tends to grow slowly, this neoplasm is associated with a poor prognosis compared to most other malignant salivary gland tumors.[1,4] The morphologic growth patterns observed in ACC of the salivary glands can be categorized into 3 types: cribriform, tubular and solid. Solid areas of the tumor usually exhibit more anaplasia and mitotic activity than do typical cribriform or tubular areas. Much evidence shows that the tubular or cribriform pattern dominant subtypes have a much better prognosis than those with predominantly solid patterns.[5–7] The prognosis of ACC is frequently unpredictable by histologic findings alone, however, especially when dealing with inadequate biopsy material.[4,8] There is a need to explore additional parameters for predicting the prognosis of ACC.

Two-dimensional (2-D) gel electrophoresis is a well-established technique that simultaneously separates and displays hundreds to thousands of proteins.[9] The method separates proteins in 2 dimensions according to their isoelectric point and molecular size. Traditionally, identification of statistically significant differences between 2 or more proteomes by 2-D gel electrophoresis required the running and analysis of many gels. The reproducibility of comparing proteomes by this method is hindered, however, by technical variations in sample preparation and gel-running conditions. Matching protein spots across different gels can become increasingly difficult when the patterns differ markedly or when only subtle changes in minor proteins are present. Such factors make it difficult to distinguish between artifactual and technical variations and biologic differences. An effective approach to reduce gel-to-gel variation is to standardize the 2-D gel results by incorporating a protein standard on every gel used in the experiment. Recently described fluorescent 2-D differential in-gel electrophoresis (2-D-DIGE)[10–13] allows multiplex analysis of 3 sample proteomes on the same gel. The protein extracts being compared are covalently labeled with different fluorescent CyDyes, which are *N*-hydroxy succinimidyl ester derivatives of Cy2, Cy3 and Cy5. Fluorescent imaging of the gel at the wavelengths specific to each CyDye generates images that can be overlaid directly by the DeCyder software to identify any differentially expressed proteins between the samples.

We examined the protein expression in ACC xenograft and normal salivary glands (NSG) using 2-D-DIGE and matrix-assisted laser desorption/ionization time-of-flight (MALDI-TOF) mass spectrometry to identify specific markers of ACC.

Material and methods

Sample preparation

We used a human tumor line derived from ACC that is serially transplantable in nude mice. Transplantations were carried out as described previously.[14] Briefly, the original tumor tissue, which was obtained from operated material of a 48-year-old male patient with ACC of the oral floor, was cut into approximately 2×2 mm pieces and transplanted into the flank of the female nude mice. The length (L) and width (W) of the tumor formed at the transplanted site were measured once a week, and the relative tumor weight was calculated as $W^2 \times L \times ½$, according to the method of Battelle Columbus Laboratories.[15] ACC tumor tissue was excised and snap frozen in liquid nitrogen. NSG that were diagnosed histologically as free from tumor cells, were obtained from 5 oral cancer patients at the time of surgical resection at Chiba University Hospital after informed consent was obtained from the patients. The study protocol was reviewed and approved by the institutional review board of Chiba University. NSG were mixed as a control after protein extraction. ACC xenograft and NSG were washed in cold PBS. Samples were crushed by liquid nitrogen and resuspended in lysis buffer (7 M urea, 2 M thiourea, 4% w/v CHAPS, 10 mM Tris pH 8.0). Insoluble material was removed by

Abbreviations: ACC, adenoid cystic carcinoma; 2-D-DIGE, 2-dimensional differential in-gel electrophoresis; MALDI-TOF, matrix-assisted laser desorption/ionization time-of-flight; NSG, normal salivary gland; PBS, phosphate buffered saline; PMF, peptide mass fingerprinting; SDS-PAGE, sodium dodecylsulfate-polyacrylamide gel electrophoresis.

Grant sponsor: Ministry of Education, Science, Sports, and Culture of Japan; Grant number: 15592096.

***Correspondence to:** Department of Clinical Molecular Biology, Graduate School of Medicine, Chiba University, 1-8-1 Inohana, Chuo-ku, Chiba 260-8670, Japan. Fax: +81-43-226-2151.
E-mail: uzawak@faculty.chiba-u.jp

Received 18 February 2005; Accepted after revision 4 May 2005
DOI 10.1002/ijc.21318
Published online 10 August 2005 in Wiley InterScience (www.interscience.wiley.com).

centrifugation at 13,000*g* for 20 min at 10°C. The protein concentration was determined using a commercial Bradford reagent (Bio-Rad, Richmond, CA). The model proteins were dissolved in lysis buffer to obtain stock solutions with final concentrations of 1 mg/ml, which were used to prepare the experimental samples.

Sample labeling

The pooled standard sample was prepared by pooling protein from each of the samples before labeling. A 1-mM stock of each dye was diluted 1:5 with anhydrous dimethyl formamide just before the labeling reaction. Approximately 50 μg of each protein extract (in 4 μl) was mixed with 1 μl of CyDye Cy2, Cy3 or Cy5 (0.2 mM) (Amersham Bioscience, Buckinghamshire, UK), vortexed and incubated on ice for 30 min in the dark as described previously by Skynner *et al.*[13] The reaction was quenched by the addition of 10 mM lysine (1 μ/400 pmol dye) followed by incubation on ice for another 10 min.

Two-dimensional gel electrophoresis

Before isoelectric focusing, pooled Cy2-labeled extracts were combined with the Cy3-labeled sample extracts and Cy5-labeled extracts according to the experimental design (Table I). The combined labeled samples were added to an equal volume of 2× sample buffer (7 M urea, 2 M thiourea, 4% w/v CHAPS, 2% v/v Pharmalytes pH 3-10), vortexed and incubated on ice in the dark for another 10 min. In addition, the volume of the combined labeled samples was adjusted to 450 μl with standard rehydration buffer (7 M urea, 2 M thiourea, 4% w/v CHAPS, 1% v/v Pharmalytes pH 3-10). Immobiline DryStrips (pH 3-10 NL, 24 cm) (Amersham Bioscience) were rehydrated overnight in the 450-μl rehydration buffer overlaid with 2.5 ml DryStrip cover fluid (Amersham Bioscience), in an Immobiline DryStrip reswelling tray (Amersham Bioscience).

Isoelectric focusing was carried out at 500 V for 500 Vh, 1,000 V for 1,000 Vh and 8,000 V for 64,000 Vh at 20°C at a maximum current setting 50 μA/strip in an IPGphor II isoelectric focusing unit (Amersham Bioscience). Before sodium dodecylsulfate-polyacrylamide gel electrophoresis (SDS-PAGE), each strip was equilibrated with 10 ml equilibration buffer A (6 M urea, 100 mM Tris-HCl pH 8.0, 30% v/v glycerol, 2% w/v SDS, 0.5% w/v DTT) on a rocking table for 15 min, followed by 10 ml equilibration buffer B (6 M urea, 100 mM Tris-HCl pH 8.0, 30% v/v glycerol, 2% w/v SDS, 4.5% w/v iodoacetamide) for another 15 min.

The strips then were loaded and run on 12% acrylamide isocratic Laemmli gels[16] using the Ettan DALT 6 apparatus (Amersham Bioscience). Gels were run at 2.5 W/gel for 30 min and then increased to 100 W after the proteins migrated into the resolving gel. The gel electrophoresis run was terminated once the bromophenol blue dye (Amersham Bioscience) migrated off the bottom of the gel at 20°C.

Image acquisition and analysis

Labeled proteins were visualized using the Typhoon 9400 imager (Amersham Bioscience). The Cy2 images were scanned using a 488-nm laser and an emission filter of 520-nm band pass (BP) 40. Cy3 images were scanned using a 532-nm laser and an emission filter of 580 nm BP30. Cy5 images were scanned using a 633-nm laser and an emission filter of 670 nm BP30. The narrow BP emission filters ensure negligible cross-talk between fluorescence channels. All gels were scanned at 100 μm resolution. Images were cropped to remove areas extraneous to the gel image using ImageQuant V 5.2 (Amersham Bioscience) before analysis.

The gel images were analyzed automatically using the DeCyder Batch Processor and DIA (differential in-gel analysis) software module (Amersham Bioscience). On individual gels, Cy2-labeled images (pooled standard) were compared to either the Cy3 or Cy5 images from the individual ACC and NSG tissues using the DeCyder-DIA software. Images from separate gels were compared using the DeCyder-BVA (biological variation analysis) software

TABLE I – EXPERIMENTAL DESIGN FOR 2-D-DIGE[1]

Gel	Cy2	Cy3	Cy5
1	Pooled standard	ACC	NSGs
2	Pooled standard	ACC	NSGs
3	Pooled standard	NSGs	ACC

[1]Approximately 50 μg of each extract and the pooled standard were labeled with the indicated CyDye, mixed, and subjected to electrophoresis on 2-D gel.

(Amersham Bioscience) to match gels using the Cy2-labeled pooled standard on each gel to normalize the images. The estimated number of spots for each codetection procedure was set to 3,000. When calculating the abundance ratios for spot pairs in codetected sample images, the spot volumes of the component spot maps must be normalized to compensate for differences in system gain (different laser intensity, fluorescence, filter transmittance, sample amount). Gel-to-gel matching of the standard spot maps from each gel followed by statistical analysis of the changes in protein abundance between samples then was carried out using the DeCyder-BVA software module. The statistical significance of each expression level was calculated using the Student's *t*-test on the logged ratios. This analysis is equivalent to doing a paired *t*-test and has increased power by accounting for the pairing of samples within gels. Protein spot expression levels, which showed a statistically significant ($p < 0.001$) increase or decrease on every gel used in our study, was accepted as being differentially expressed between the extracts under comparison.

MALDI-TOF peptide mass fingerprinting analysis and database searching

Separate preparative gels electrophoresed with individual ACC and NSG tissues were fixed and stained with SYPRO Ruby (Molecular Probes, Inc., Eugene, OR). The resulting fluorescent images were matched to CyDye images using DeCyder software. A spot-picking list was generated from DeCyder and exported to an automated spot handling system, Ettan Spot Picker (Amersham Bioscience). The spot picker transferred the pixel information from DeCyder software to x-y coordinates in conjunction with the reference markers. The gel spots were excised as circular plugs 2 mm in diameter and delivered into 96-well microtiter plates.

The protein spots were excised from the gels and in-gel digestion was carried out with an enzyme solution containing 50 mM NH_4HCO_3, 5 mM $CaCl_2$ and 12.5 ng/μl trypsin. Aliquots of the purified samples were spotted on matrix crystals of μ-cyano-4-hydroxyl-cinnamic acid on a stainless steel target and air dried. Mass determinations were carried out on the AXIMA-CFR mass spectrometer (Shimadzu Co. Ltd., Kyoto, Japan). The proteins were identified by the peptide mass fingerprinting (PMF) method, using Mascot Search on the Web (http://www.matrixscience.com/cgi/index.pl?page=../home.html) (Matrix Science, Ltd., London).

Western blot analysis

Of the upregulated proteins in ACC tissue identified by mass spectrometry, 2 were selected for further analyses: maspin, which was reported to have a peculiar role as a tumor suppressor, and stathmin, which is also referred to as oncoprotein18, leukemia-associated phosphoprotein p18.

To investigate maspin and stathmin protein expression in NSG and ACC tissues, we carried out Western blot analysis. A small portion of the protein lysates of NSG and ACC, which underwent 2-D-DIGE analysis, were used. Furthermore, protein of clinical ACC tissue, obtained from a patient at the time of surgical resection at Chiba University Hospital after informed consent was provided, was extracted as described previously. Protein extracts were electrophoresed on 11% SDS-PAGE gels, transferred to PVDF membranes (Bio-Rad, Hercules, CA) and blocked for 1 hr at room temperature in 5% skim milk. Immunoblot PVDF membranes were washed with 0.1% Tween 20 in TBS (TBS-T) 5 times, and

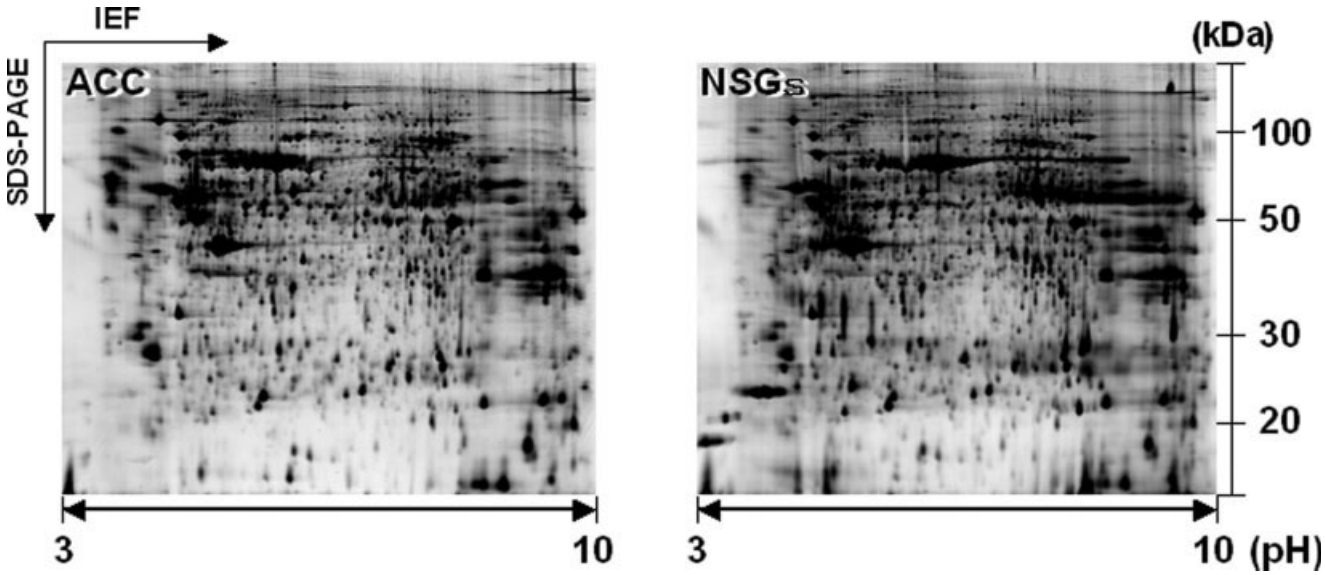

FIGURE 1 – Typical 2-D-DIGE gel images of ACC and NSG. The protein lysates were labeled with either Cy3 or Cy5 and subjected to 2-D-DIGE using pH 3-10 IPG strips.

TABLE II – PROTEIN DIFFERENTIALLY EXPRESSED IN ACC COMPARED WITH NSG

Accession	Protein name[1]	Theoretical pl/Mw (kDa)	*t*-test	Average ratio
gil 5031851	Stathmin	5.7/17.3	8.70e-05	8.53
gil 4505789	Maspin	5.7/42.6	4.10e-05	8.46
gil 223002	Fibrin beta	7.95/51.3	0.00039	4.87
gil 14164615	SIGLEC 8	7.5/44.8	8.60e-05	3.35
gil 12707570	ECHS 1	8.3/31.8	7.20e-06	−4.13
gil 13489087	SERPIN B1	5.9/42.8	0.00078	−5.86
gil 2780818	SOD2	6.9/22.3	2.60e-06	−6.18
gil 47077495	ALAD	7.6/39.6	1.20e-05	−6.52
gil 178775	Proapolipoprotein	5.4/28.9	2.50e-05	−26.73

[1]SIGLEC 8, sialic acid binding immunoglobulin-like lectin 8; ECHS 1, enoyl Coenzyme A hydratase short chain 1; SERPIN B1, serine proteinase inhibitor clade B member 1; SOD 2, superoxide dismutase 2; ALAD, aminolevulinate delta-dehydratase.

2 μg/ml affinity-purified goat antihuman maspin polyclonal antibody (Santa Cruz Biotechnology, Santa Cruz, CA) and 2 μg/ml affinity-purified goat antihuman stathmin polyclonal antibody (Santa Cruz Biotechnology) were added directly to the TBS-T solution for 2 hr at room temperature. PVDF membranes were washed again and incubated with a 1:10,000 of HRP-conjugated anti-goat IgG Ab (Santa Cruz Biotechnology) as a secondary antibody for 20 min at room temperature. Finally, membranes were incubated with ECL+-horseradish peroxidase substrate solution included in the ECL+ kit (Amersham Bioscience), and immunoblotting was visualized by exposing the membrane to Hyperfilm (Amersham Bioscience).

Immunohistochemistry

To examine the cellular distribution of maspin and stathmin in normal and neoplastic salivary gland including ACC, we carried out immunohistochemical staining of salivary gland tumors, 10 cases of pleomorphic adenoma (PA), 10 cases of ACC and 2 cases of NSG. The tissue was obtained at the time of surgical resection at Chiba University Hospital after informed consent was obtained from the patients according to a protocol that was reviewed and approved by the institutional review board of Chiba University. Briefly, the 4-μm paraffin-embedded specimen was deparaffinized and hydrated. The slides were treated with endogenous peroxidase in 0.3% hydrogen peroxide for 30 min and the sections were blocked for 2 hr at room temperature with 1.5% blocking serum (Santa Cruz Biotechnology) in PBS before reacting with antihuman maspin polyclonal antibody (Santa Cruz Biotechnology) and antihuman stathmin polyclonal antibody (Santa Cruz Biotechnology) at a dilution of 1:100. They were then incubated with primary antibody and nonimmune control antibody for 3 hr at room temperature in a moist chamber. After incubation, samples were incubated with biotinylated anti-goat IgG and peroxidase-conjugated streptavidin. The peroxidase reaction was carried out using a 3,3′-diaminobenzidine tetrahydrochloride (DAKO Japan Inc., Kyoto, Japan). The slides were counterstained with hematoxylin, dehydrated in graded ethanol, cleaned in xylene and mounted.

Results

Proteomics analysis of differentially expressed proteins between ACC and normal tissue by 2-D-DIGE

To identify specific markers of ACC, we used 2-D-DIGE technology to monitor changes in the abundance of proteins. Table I shows the CyDye labeling and gel running design. The proteins were separated by isoelectric focusing on pH 3-10 Immobiline DryStrips followed by 12% SDS-PAGE in the second dimension. The samples were run in triplicate to obtain the statistical significance of protein differences. Figure 1 shows that an average of about 2,500 spots was detected across all 3 gels by the DeCyder software. Computer-assisted comparative analysis using the BVA mode of the DeCyder software showed 4 protein spots that were more than 3-fold upregulated and 5 protein spots that were more than 3-fold downregulated in intensity in ACC tissues compared to NSG tissues ($p < 0.001$) (Table II).

MALDI-TOF PMF analysis

Based on the comparative analysis of protein expression patterns between ACC and NSG tissue, the 9 differentially expressed proteins were selected for further analysis. To identify these spots, we ran separate preparative gels containing 300 μg of each extract, which were post-stained by SYPRO Ruby. All protein spots were matched to the CyDye labeled images by the DeCyder software (data not shown). These spots were robotically excised from the gels for MALDI-TOF PMF analysis. All were specifically digested by trypsin and peptide masses maps were obtained from PMF analysis. Nine known proteins were extracted from the analysis.

Identification of the proteins by MALDI-TOF PMF analysis

We identified 4 proteins upregulated in ACC 9 (*i.e.*, stathmin, maspin, fibrin beta, sialic acid binding immunoglobulin-like lectin 8 [SIGLEC 8]) and 5 proteins downregulated in ACC (*i.e.*, enoyl coenzyme A hydratase short chain 1 [ECHS 1], serin proteinase inhibitor B 1 [SERPIN B1], superoxide dismutase 2 [SOD 2], aminolevulinate delta-dehydratase [ALAD], pro-apolipoprotein) (Table II). Of the upregulated proteins in ACC tissues, which were >5-fold upregulated, 2 were selected for further analyses: maspin, which has a peculiar role as a tumor suppressor, and stathmin, also referred to as oncoprtein18, leukemia-associated phosphoprotein p18. The typical results of Decyder software for maspin and stathmin protein spots are shown in Figure 2*a*,*b*. The 3-D peak of a protein spot was generated based on the pixel *vs*. area data from the images obtained by the 2-D Master Imager. The peak area showed the distribution of the protein spot in the gel, whereas the volume correlated with the amount of protein. We detected overexpression of these proteins in 2-D and 3-D images of ACC tissue. We did not detect these protein spots in the NSG. tissue. In our study, the differences in protein expression were detected more easily by the DeCyder 3-D spot simulations. Figure 3 shows the results of PMF analysis for maspin and stathmin.

Confirmation of maspin and stathmin by Western blot analysis

To ensure that maspin and stathmin were truly overexpressed in ACC, we carried out Western blot analysis. Figure 4 shows representative results. Maspin and stathmin protein expression was found to be significantly increased in ACC xenograft. In addition, these proteins were also significantly overexpressed in clinical ACC tissue. Western blotting experiments confirmed the results from 2-D gel analysis and protein identification by mass spectrometry.

Immunohistochemical expression of maspin and stathmin in normal and neoplastic salivary gland

To investigate the distribution of maspin and stathmin protein expression in normal and neoplastic salivary gland including ACC, we carried out immunohistochemical staining of the protein in 2 cases with NSG, 10 cases of PA and 10 cases of ACC. All specimens studied were positive for maspin and stathmin in different degrees.

Figure 5 shows representative staining results of maspin. Myoepithelial cells lining the acini periphery were positive for maspin in NSG tissue (Fig. 5*a*). In PA, maspin was very abundant in highly cellular areas, although not all cells were positive (Fig. 5*b*). Luminal and myoepithelial cells were strongly positive for maspin in the tubular type of ACC (Fig. 5*c*). Only a few cells lining the duct-like structures were positive for maspin in the cribriform type of ACC (Fig. 5*d*). In the solid type of ACC, only a few cells in the core region of the nests were positive for maspin (Fig. 5*e*).

Figure 6 shows representative staining results for stathmin. In NSG tissue, there was no staining for stathmin (Fig. 6*a*). Stathmin was present in a few nonluminal cells in PA (Fig. 6*b*). Only a few cells were positive for stathmin in the tubular type of ACC (Fig. 6*c*). Luminal cells and a few cells lining the duct-like structures were positive for stathmin in the cribriform type of ACC (Fig. 6*d*). Luminal and myoepithelial cells were strongly positive for stathmin in the solid type of ACC (Fig. 6*e*).

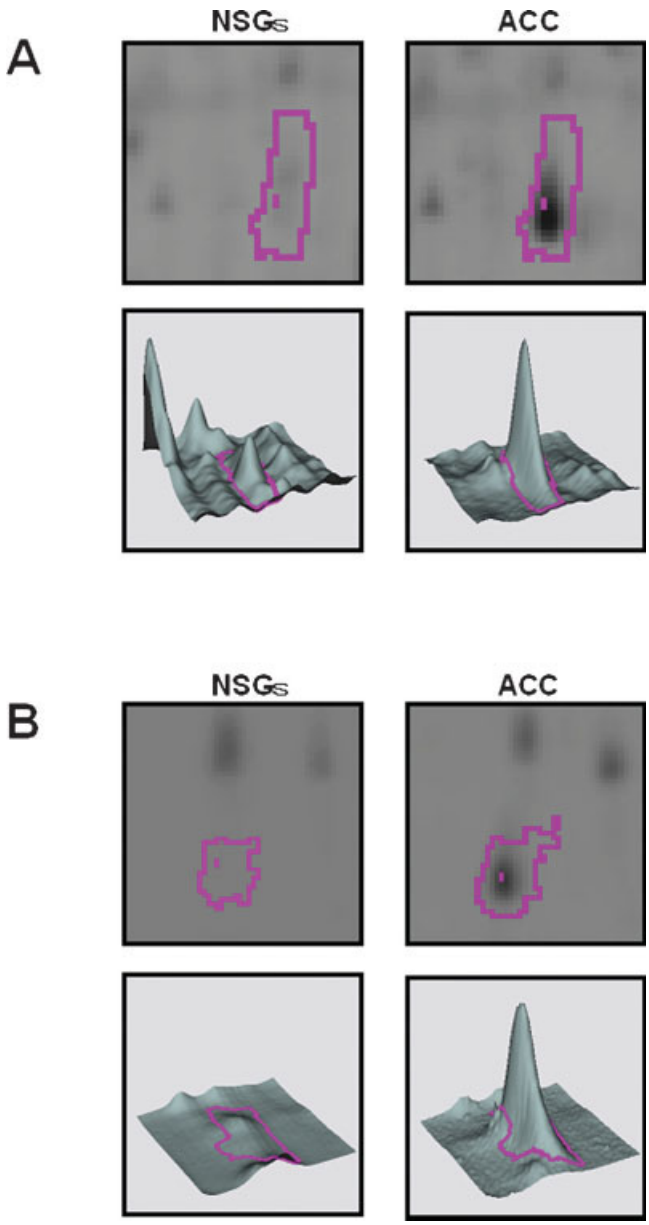

Figure 2 – Typical results of protein expression in ACC and NSG using DeCyder software. (*a*) The maspin protein expression levels in ACC are significantly higher than that in NSG. (*b*) The stathmin protein expression levels in ACC are also significantly higher.

Discussion

Because the functional molecules in the cell are protein, proteome analysis based on 2-D gel electrophoresis is believed to have several advantages over cDNA/oligonucleotide microarray systems for clinical use. First, the system measures primarily high-abundance proteins, which are ideal specific biomarkers because they can be easily measured and targeted. mRNA levels are not directly associated with the amounts of functional proteins.[17] Although studies at the mRNA level are capable of rapidly assessing the expression profiles of a large number of transcripts, this kind of analysis measures only the relative abundance of an mRNA encoding a protein and not the actual protein abundance in the disease lesion. Second, using proteomics, we can analyze the post-translational modifications such as acetylation, ubiquitina-

A

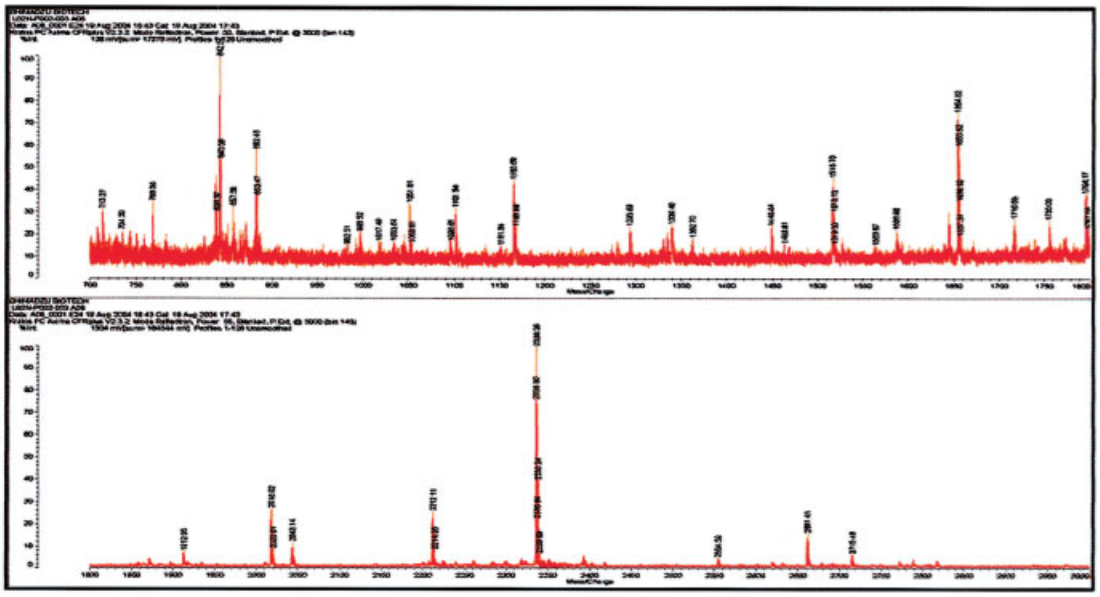

B

1 MDALQLANSA FAVDLFKQLC EKEPLGNVLF SPICLSTSLS LAQVGAKGDT

51 ANEIGQVLHF ENVKDIPFGF QTVTSDVNKL SSFYSLKLIK RLYVDKSLNL

101 STEFISSTKR PYAKELETVD FKDKLEETKG QINNSIKDLT DGHFENILAD

151 NSVNDQTKIL VVNAAYFVGK WMKKFPESET KECPFRLNKT DTKPVQMMNM

201 EATFCMGNID SINCKIIELP FQNKHLSMFI LLPKDVEDES TGLEKIEKQL

251 NSESLSQWTN PSTMANAKVK LSIPKFKVEK MIDPKACLEN LGLKHIFSED

301 TSDFSGMSET KGVALSNVIH KVCLEITEDG GDSIEVPGAR ILQHKDELNA

351 DHPFIYIIRH NKTRNIIFFG KFCSP

C

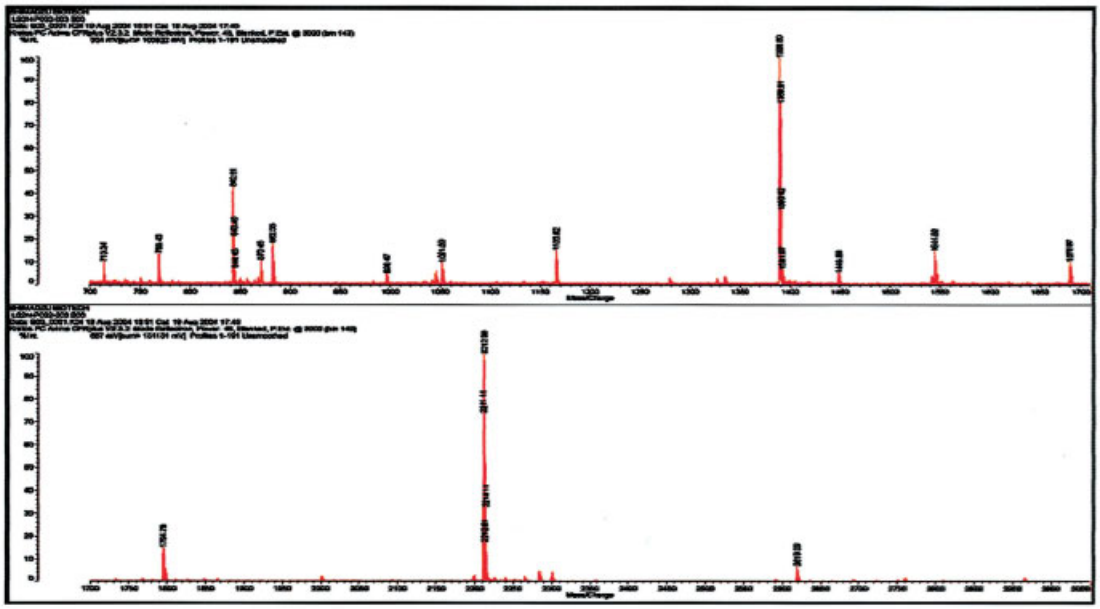

D

1 MASSDIQVKE LEKRASGQAF ELILSPRSKE SVPEFPLSPP KKKDLSLEEI

51 QKKLEAAEER RKSHEAEVLK QLAEKREHEK EVLQKAIEEN NNFSKMAEEK

101 LTHKMEANKE NREAQMAAKL ERLREKDKHI EEVRKNKESK DPADETEAD

FIGURE 3

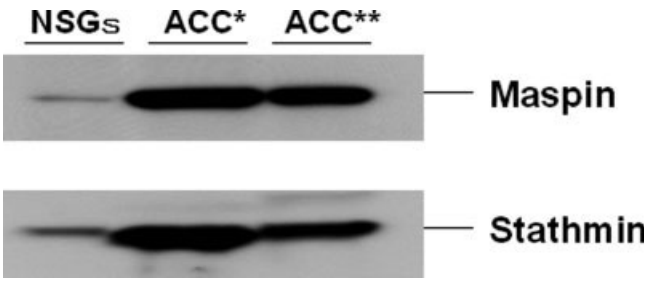

FIGURE 4 – Representative results of expression of maspin and stathmin protein in NSG and ACC tissues. To investigate maspin and stathmin protein expression in NSG and ACC, including clinical tissue of ACC, we carried out Western blot analysis. The size of the maspin protein band is 42 kDa, and the size of the stathmin protein band is 17 kDa. *Maspin and stathmin protein expression is significantly increased in ACC xenograft. **In addition, these proteins are also significantly overexpressed in clinical ACC tissue.

tion, phosphorylation, or glycosylation that are essential for protein formation and function.[18,19] For many proteins, post-translational modifications are important for their function, and they can be analyzed only by the methods used in proteomics.[20,21] The proteomic results express the intrinsic genetic effect on cell and the impact of its environment. It is therefore very valuable to determine biomarkers.

Our present study showed that 2-D-DIGE is a robust method to identify statistically significant changes in protein abundance between tumor and normal tissue. The technique provides reliable identification of proteomic differences between the samples, because multiple samples can be analyzed on a single gel and an internal standard can be included for accurate matching across gels.[22] The use of an internal standard helps to minimize false positives and negatives, because it provides separate control for each individual protein spot on all gels in the analysis.[22] It is possible that the CyDyes may show some artifactual preferential labeling of some proteins, although we did not detect any.

To investigate the proteins differentially expressed in ACC and NSG tissues, and especially to identify specific markers of ACC, we carried out 2-D-DIGE analysis. As shown in Table II, we identified 4 proteins upregulated in ACC and 5 proteins downregulated in ACC. Of the upregulated proteins, maspin has a peculiar role as tumor suppressor,[23] stathmin regulates the dynamics of microtubule polymerization and depolymerization,[24] fibrin beta may affect the progression of tumor cell growth and metastasis,[25] SIGLEC8 is a novel eosinophil-specific member of the immunoglobulin superfamily. Of the downregulated proteins in ACC, ECHS1 catalyzes the mitochondrial fatty acid b-oxidation,[26] SERPINB1 is one of the most efficient inhibitor of the neutrophil granule proteases, SOD2 is related to the cellular defense response,[27] ALAD is related to the heme synthesis[28] and pro-apolipoprotein has functions of the transport of cholesterol and the formation of high density lipoprotein (HDL). Of them, SOD2 is reported as a candidate tumor suppressor,[29–31] downregulation of ECHS1 is associated with doxorubicin chemo-resistance of hepatocellular carcinoma.[32] Proapolipoprotein showing a significant downregulation in ACC is hydrolyzed by the signal peptidase and propeptidase, through which apolipoprotein is generated.[33] Apolipoprotein is a carrier of lipids and regulates many cellular functions. It was found that apolipoprotein had an anti-apoptosis effect and was related with carcinogenesis and progression. Enhanced expression of apolipoprotein has been reported in hepatoma[34] and colorectal cancer.[35] To date, there is no report regarding downregulation of pro-apolipoprotein in human cancers, with the exception of ACC used in our study, suggesting that this protein may play a different role between ACC and other types of malignant tumors.

Of the proteins expressed differentially in ACC and NSG tissues, maspin and stathmin were remarkably upregulated (>5-fold) in ACC. Western blotting experiments confirmed the results from 2-D gel analysis and protein identification by mass spectrometry. Maspin is a member of the serpin superfamily of protease inhibitors, and it has a peculiar role as a tumor suppressor.[23] The maspin gene was identified originally by Zou *et al*.[36] in normal mammary epithelium by subtractive hybridization on the basis of its expression at the mRNA level. Maspin has tumor-suppressive activity attributed to inhibition of breast cancer cell motility, invasion and metastasis.[37–39] Loss of maspin protein expression has been observed frequently and is associated with poor prognosis in breast, prostatic and oral cancers.[40–42] A recent study suggested that maspin interacts with the p53 tumor suppressor pathway and may inhibit angiogenesis[43] *in vitro* and *in vivo*. These observations suggest that maspin acts as a tumor suppressor gene. Maspin seems to behave as an oncogene rather than a tumor suppressor gene in pancreatic[44] and ovarian[45] cancers. Sood *et al*.[45] reported that patients with invasive ovarian cancer exhibiting maspin upregulation have a poor prognosis.

In our present study, maspin was overexpressed in ACC tissue compared to NSG tissue. Furthermore, we detected maspin protein expression in 2 cases with NSG, 10 cases of PA, and 10 cases of ACC using immunohistochemistry (Fig. 5). In PA, maspin was very abundant in highly cellular areas, whereas only myoepithelial cells lining the acini periphery were positive for maspin in NSG. Among the 3 histologic patterns of ACC (tubular, cribriform, solid), the tubular subtype showed abundant maspin staining, whereas only a few cells in the core region of the nests were positive for maspin in the solid subtype. In addition, only a few cells lining the duct-like structures were positive for maspin in the cribriform type of ACC. De Lima Navarro *et al*.[46] reported that maspin expression in these neoplasms coincides with biologic behavior, *i.e*., the more aggressive histologic types had fewer positive cells. Much evidence shows that histologic ACC subtypes are directly related to prognosis, with the tubular pattern having the best prognosis and the solid type the worst prognosis.[47,48] Our findings agree with this biologic behavior. Maspin is an important marker of biologic behavior in ACC of the salivary gland.

Stathmin, also called oncoprotein 18/Op18, leukemia-associated phosphoprotein p18, is a member of a novel class of microtubule-destabilizing proteins that regulates the dynamics of microtubule polymerization and depolymerization.[24] Stathmin promotes microtubule depolymerization during interphase and late mitosis. This microtubule depolymerizing activity of stathmin is regulated by changes in its level of phosphorylation that occur during cell cycle progression.[49] These modifications allow it to play a critical role in the regulation of the dynamic equilibrium of microtubules during different phases of the cell cycle. Because it can be differently phosphorylated in response to hormones,[50] growth factors[51] or neurotransmitters,[52] stathmin is thought to integrate diverse intracellular signaling pathways[53] that may interfere with various microtubule-dependent cellular functions.[54,55] Stathmin is expressed at high levels in a wide variety of human malignancies.[56–59]

We identified overexpression of stathmin in ACC tissue. Further, we detected stathmin protein expression in 2 cases with

FIGURE 3 – MALDI-TOF mass spectrometric analysis of maspin and stathmin, which were expressed more frequently in ACC. (*a*) Results of MALDI-TOF mass spectrometric analysis of maspin. (*b*) Amino acid sequences analyzed for maspin by PMF analysis and underlined in the full-length sequence of the protein. (*c*) Results of MALDI-TOF mass spectrometric analysis of stathmin. (*d*) Amino acid sequences analyzed for stathmin by PMF analysis and underlined in the full-length sequence of the protein.

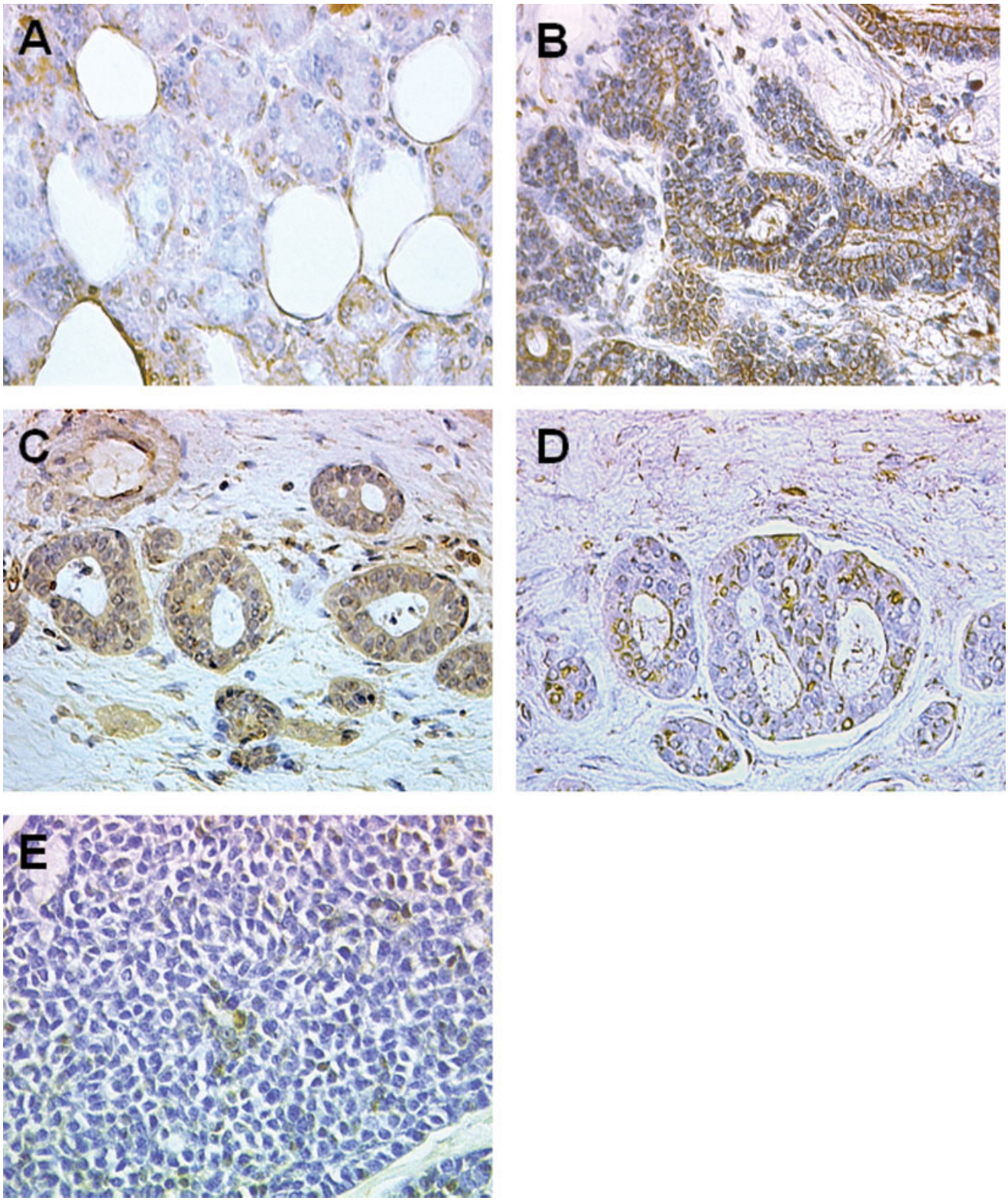

FIGURE 5 – Immunohistochemical staining of maspin protein in normal and neoplastic salivary gland, PA and ACC. Magnification = 400×. (*a*) Myoepithelial cells lining the acini periphery are positive for maspin in normal salivary gland. (*b*) In PA, maspin is very abundant in highly cellular areas. (*c*) Luminal and myoepithelial cells are strongly positive for maspin in the tubular type of ACC. (*d*) Only a few cells lining the duct-like structures are positive for maspin in cribriform type of ACC. (*e*) Only a few cells in the core region of the nests are positive for maspin in the solid type of ACC.

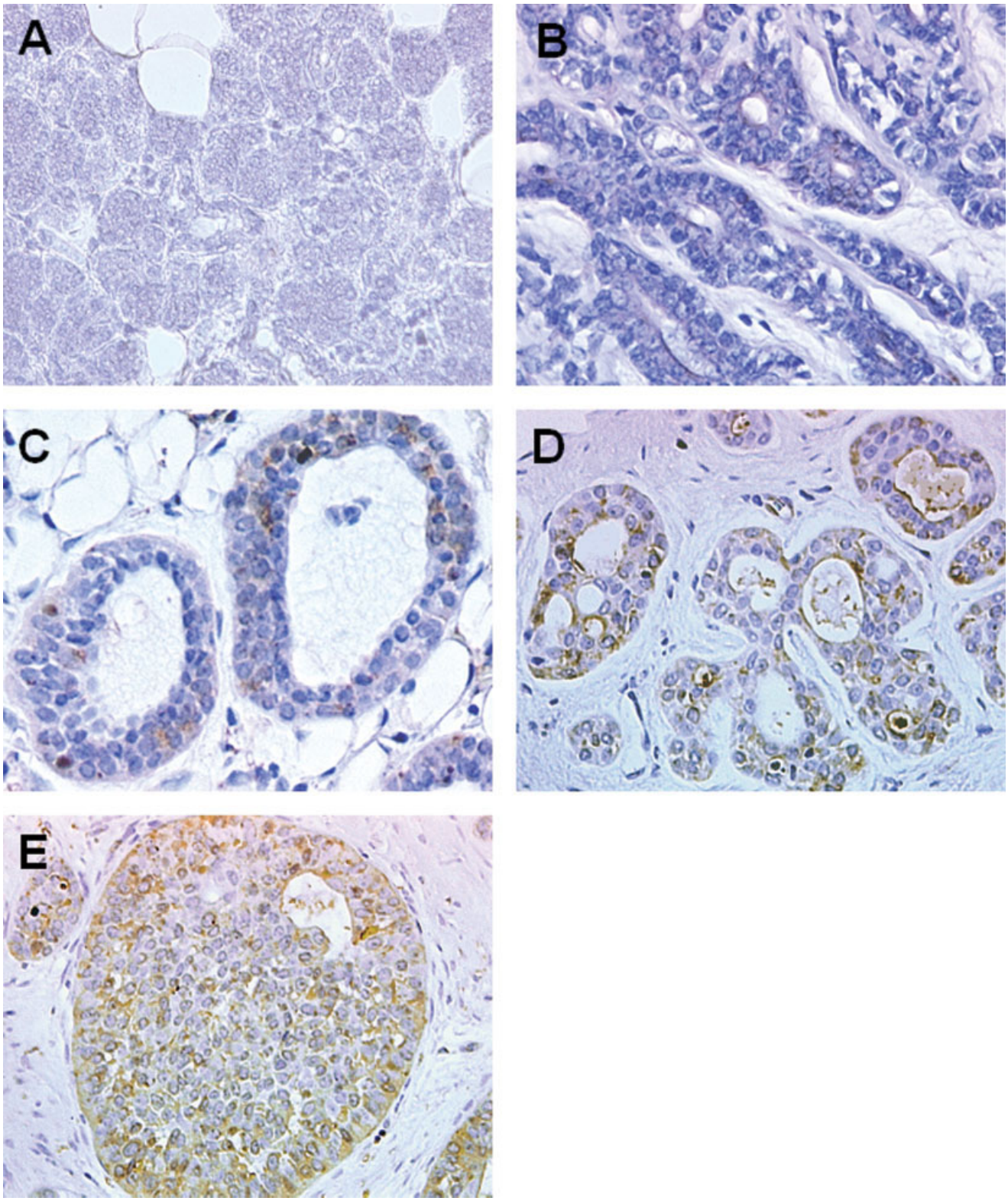

FIGURE 6 – Immunohistochemical staining of stathmin protein in normal and neoplastic salivary gland, PA and ACC. Magnification = 400×. (*a*) No staining for stathmin is seen in NSG tissue. (*b*) Stathmin is present in a few nonluminal cells in PA. (*c*) Only a few cells are positive for stathmin in the tubular type of ACC. (*d*) Luminal cells and a few cells lining the duct-like structures are positive for stathmin in the cribriform type of ACC. (*e*) Luminal and myoepithelial cells are strongly positive for stathmin in the solid type of ACC.

NSG, 10 cases of PA and 10 cases of ACC using immunohistochemistry (Fig. 6). Although no staining was seen in NSG and only a few cells were positive for stathmin in PA, all 3 variants of ACC were positive for stathmin. In addition, among the 3 histologic patterns of ACC, the solid subtype showed abundant stathmin staining, whereas a few luminal cells were positive for stathmin in the

tubular subtype. These results show a significant correlation between histologic grading and stathmin expression. Because much evidence shows that ACC histologic subtypes are directly related to prognosis, with the tubular pattern presenting the best prognosis and the solid type the worst prognosis,[47,48] these findings suggest that the expression of stathmin protein may affect the prognosis of ACC.

In summary, we used 2-D-DIGE technology to identify specific markers of ACC. Significant over- or underexpressed proteins were found in ACC tissue. In particular, because different expression patterns between maspin and stathmin were detected among the subtypes of ACC, we suggest that these proteins may be not only useful biomarkers of ACC but also markers of biologic behavior in this tumor.

Acknowledgements

We thank L.C. Charters for proofreading this manuscript.

References

1. Spiro RH, Huvos AG, Strong EW. Adenoid cystic carcinoma of salivary origin. A clinicopathologic study of 242 cases. Am J Surg 1974; 128:512–20.
2. Chilla R, Schroth R, Eysholdt U, Droese M. Adenoid cystic carcinoma of the head and neck. Controllable and uncontrollable factors in treatment and prognosis. ORL J Otorhinolaryngol Relat Spec 1980; 42:346–67.
3. Szanto PA, Luna MA, Tortoledo ME, White RA. Histologic grading of adenoid cystic carcinoma of the salivary glands. Cancer 1984;54: 1062–9.
4. Peel RL, Gnepp DR. Disease of the salivary glands. In: Barnes L, ed. Surgical pathology of the head and neck. New York: Dekker, 1985. p 533–45.
5. Chomette G, Auriol M, Tranbaloc P, Vaillant JM. Adenoid cystic carcinoma of minor salivary glands: analysis of 86 cases. Clinicopathological, histoenzymological and ultrastructural studies. Virchows Arch A Pathol Anat 1982;395:289–301.
6. Batsakis JG, Luna MA, El-Naggar A. Histopathologic grading of salivary gland neoplasms: III. Adenoid cystic carcinomas. Ann Otol Rhinol Laryngol 1990;99:1007–9.
7. Goepfert H, Luna MA, Lindberg RD, White AK. Malignant salivary gland tumors of the paranasal sinuses and nasal cavity. Arch Otolaryngol 1983;109:662–8.
8. Vuhahula EA, Nikai H, Ogawa I, Miyauchi M, Takata T, Ito H, Ito R. Correlation between argyrophilic nucleolar organizer region (AgNOR) counts and histologic grades with respect to biologic behavior of salivary adenoid cystic carcinoma. J Oral Pathol Med 1995;24: 437–42.
9. O'Farrell PH. High resolution two-dimensional electrophoresis of proteins. J Biol Chem 1975;250:4007–21.
10. Unlu M, Morgan ME, Minden JS. Difference gel electrophoresis: a single gel method for detecting changes in protein extracts. Electrophoresis 1997;18:2071–7.
11. Tonge R, Shaw J, Middleton B, Rowlinson R, Rayner S, Young J, Pognan F, Hawkins E, Currie I, Davison M. Validation and development of fluorescence two-dimensional differential gel electrophoresis proteomics technology. Proteomics 2001;1:377–96.
12. Zhou G, Li H, DeCamp D, Chen S, Shu H, Gong Y, Flaig M, Gillespie JW, Hu N, Taylor PR, Emmert-Buck MR, Liotta LA, et al. 2D differential in-gel electrophoresis for the identification of esophageal scans cell cancer-specific protein markers. Mol Cell Proteomics 2002;1: 117–24.
13. Skynner HA, Rosahl TW, Knowles MR, Salim K, Reid L, Cothliff R, McAllister G, Guest PC. Alterations of stress related proteins in genetically altered mice revealed by two-dimensional differential in-gel electrophoresis analysis. Proteomics 2002;2:1018–25.
14. Hashitani S, Noguchi K, Manno Y, Moridera K, Takaoka K, Nishimura N, Kishimoto H, Sakurai K, Urade M. Changes of histological and biological features by serial passages in a human adenoid cystic carcinoma line transplantable in nude mice. Oncol Rep 2005; 13:607–12.
15. Ovejera AA, Houchens DP, Barker AD. Chemotherapy of human tumor xenografts in genetically athymic mice. Ann Clin Lab Sci 1978;8:50–6.
16. Laemmli UK. Cleavage of structural proteins during the assembly of the head of bacteriophage T4. Nature 1970;15:680–5.
17. Futcher B, Latter GI, Monardo P, McLaughlin CS, Garrels JI. A sampling of the yeast proteome. Mol Cell Biol 1999;19:7357–68.
18. Larsson T, Bergstrom J, Nilsson C, Karlsson KA. Use of an affinity proteomics approach for the identification of low-abundant bacterial adhesins as applied on the Lewis (b)-binding adhesin of Helicobacter pylori. FEBS Lett 2000;469:155–8.
19. Charlwood J, Skehel JM, Camilleri P. Analysis of N-linked oligosaccharides released from glycoproteins separated by two-dimensional gel electrophoresis. Anal Biochem 2000;284:49–59.
20. Sali A. Functional links between proteins. Nature 1999;402:25–6.
21. Oliver S. Guilt-by-association goes global. Nature 2000;403:601–3.
22. Knowles MR, Cervino S, Skynner HA, Hunt SP, de Felipe C, Salim K, Meneses-Lorente G, McAllister G, Guest PC. Multiplex proteomic analysis by two-dimensional differential in-gel electrophoresis. Proteomics 2003;3:1162–71.
23. Sheng S, Pemberton PA, Sager R. Production, purification, and characterization of recombinant maspin proteins. J Biol Chem 1994;269: 30988–93.
24. Melander Gradin H, Marklund U, Larsson N, Chatila TA, Gullberg M. Regulation of microtubule dynamics by Ca2+/calmodulin-dependent kinase IV/Gr-dependent phosphorylation of oncoprotein 18. Mol Cell Biol 1997;17:3459–67.
25. Palumbo JS, Kombrinck KW, Drew AF, Grimes TS, Kiser JH, Degen JL, Bugge TH. Fibrinogen is an important determinant of the metastatic potential of circulating tumor cells. Blood 2000;96:3302–9.
26. Janssen U, Davis EM, Le Beau MM, Stoffel W. Human mitochondrial enoyl-CoA hydratase gene (ECHS1): structural organization and assignment to chromosome 10q26.2–q26.3. Genomics 1997;40:470–5.
27. Li Y, Huang TT, Carlson EJ, Melov S, Ursell PC, Olson JL, Noble LJ, Yoshimura MP, Berger C, Chan PH, Wallace DC, Epstein CJ. Dilated cardiomyopathy and neonatal lethality in mutant mice lacking manganese superoxide dismutase. Nat Genet 1995;11:376–81.
28. Anderson PM, Desnick R. Purification and properties of delta-aminolevulinate dehydrase from human erythrocytes. J Biol Chem 1979; 254:6924–30.
29. Church SL, Grant JW, Ridnour LA, Oberley LW, Swanson PE, Meltzer PS, Trent JM. Increased manganese superoxide dismutase expression suppresses the malignant phenotype of human melanoma cells. Proc Natl Acad Sci USA 1993;90:3113–7.
30. Liu R, Oberley TD, Oberley LW. Transfection and expression of MnSOD cDNA decreases tumor malignancy of human oral squamous carcinoma SCC-25 cells. Hum Gene Ther 1997;8:585–95.
31. Zhong W, Oberley LW, Oberley TD, St. Clair DK. Suppression of the malignant phenotype of human glioma cells by overexpression of manganese superoxide dismutase. Oncogene 1997;14:481–90.
32. Hu Y, Pang E, Lai PB, Squire JA, MacGregor PF, Beheshti B, Albert M, Leung TW, Wong N. Genetic alterations in doxorubicin-resistant hepatocellular carcinoma cells: a combined study of spectral karyotyping, positional expression profiling and candidate genes. Int J Oncol 2004;25:1357–64.
33. Tricerri MA, Behling Agree AK, Sanchez SA, Jonas A. Characterization of apolipoprotein A-I structure using a cysteine-specific fluorescence probe. Biochemistry 2000;39:14682–91.
34. Nassir F, Bonen DK, Davidson NO. Apolipoprotein(a) synthesis and secretion from hepatoma cells is coupled to triglyceride synthesis and secretion. J Biol Chem 1998;273:17793–800.
35. Yu B, Li SY, An P, Zhang YN, Liang ZJ, Yuan SJ, Cai HY. Comparative study of proteome between primary cancer and hepatic metastatic tumor in colorectal cancer. World J Gastroenterol 2004;10:2652–6.
36. Zou Z, Anisowicz A, Hendrix MJ, Thor A, Neveu M, Sheng S, Rafidi K, Seftor E, Sager R. Maspin, a serpin with tumor-suppressing activity in human mammary epithelial cells. Science 1994;263:526–9.
37. Sheng S, Truong B, Fredrickson D, Wu R, Pardee AB, Sager R. Tissue-type plasminogen activator is a target of the tumor suppressor gene maspin. Proc Natl Acad Sci USA 1998;95:499–504.
38. McGowen R, Biliran H Jr, Sager R, Sheng S. The surface of prostate carcinoma DU145 cells mediates the inhibition of urokinase-type plasminogen activator by maspin. Cancer Res 2000;60:4771–8.
39. Shi HY, Zhang W, Liang R, Abraham S, Kittrell FS, Medina D, Zhang M. Blocking tumor growth, invasion, and metastasis by maspin in a syngeneic breast cancer model. Cancer Res 2001;61:6945–51.
40. Xia W, Lau YK, Hu MC, Li L, Johnston DA, Sheng S, El-Naggar A, Hung MC. High tumoral maspin expression is associated with improved survival of patients with oral squamous cell carcinoma. Oncogene 2000;19:2398–403.
41. Machtens S, Serth J, Bokemeyer C, Bathke W, Minssen A, Kollmannsberger C, Hartmann J, Knuchel R, Kondo M, Jonas U, Kuczyk M. Expression of the p53 and Maspin protein in primary prostate cancer: correlation with clinical features. Int J Cancer 2001;95:337–42.
42. Umekita Y, Ohi Y, Sagara Y, Yoshida H. Expression of maspin predicts poor prognosis in breast-cancer patients. Int J Cancer 2002; 100:452–5.

43. Zou Z, Gao C, Nagaich AK, Connell T, Saito S, Moul JW, Seth P, Appella E, Srivastava S. p53 regulates the expression of the tumor suppressor gene maspin. J Biol Chem 2000;275:6051–4.
44. Maass N, Hojo T, Ueding M, Luttges J, Kloppel G, Jonat W, Nagasaki K. Expression of the tumor suppressor gene Maspin in human pancreatic cancers. Clin Cancer Res 2001;7:812–7.
45. Sood AK, Fletcher MS, Gruman LM, Coffin JE, Jabbari S, Khalkhali-Ellis Z, Arbour N, Seftor EA, Hendrix MJ. The paradoxical expression of maspin in ovarian carcinoma. Clin Cancer Res 2002;8:2924–32.
46. Navarro de Lima R, Martins MT, de Araujo VC. Maspin expression in normal and neoplastic salivary gland. J Oral Pathol Med 2004;33:435–40.
47. Szanto PA, Luna MA, Tortoledo ME, White RA. Histologic grading of adenoid cystic carcinoma of the salivary glands. Cancer 1984;54:1062–9.
48. Santucci M, Bondi R. New prognostic criterion in adenoid cystic carcinoma of salivary gland origin. Am J Clin Pathol 1989;91:132–6.
49. Lawler S. Microtubule dynamics: if you need a shrink try stathmin/Op18. Curr Biol 1998;12:212–4.
50. Beretta L, Boutterin MC, Sobel A. Phosphorylation of intracellular proteins related to the multihormonal regulation of prolactin: comparison of normal anterior pituitary cells in culture with the tumor-derived GH cell lines. Endocrinology 1988;122:40–51.
51. Doye V, Boutterin MC, Sobel A. Phosphorylation of stathmin and other proteins related to nerve growth factor-induced regulation of PC12 cells. J Biol Chem 1990;265:11650–5.
52. Chneiweiss H, Cordier J, Sobel A. Stathmin phosphorylation is regulated in striatal neurons by vasoactive intestinal peptide and monoamines via multiple intracellular pathways. J Neurochem 1992; 58:282–9.
53. Sobel A. Stathmin: a relay phosphoprotein for multiple signal transduction? Trends Biochem Sci 1991;16:301–5.
54. Gavet O, Ozon S, Manceau V, Lawler S, Curmi P, Sobel A. The stathmin phosphoprotein family. Intracellular localization and effects on the microtubule network. J Cell Sci 1998;111:3333–46.
55. Ghosh PK, Anderson J, Cohen N, Takeshita K, Atweh GF, Lebowitz P. Expression of the leukemia-associated gene, p18, in normal and malignant tissues: inactivation of expression in a patient with cleaved B cell lymphoma/leukemia. Oncogene 1993;8:2869–72.
56. Roos G, Brattsand G, Landberg G, Marklund U, Gullberg M. Expression of oncoprotein 18 in human leukemias and lymphomas. Leukemia 1993;7:1538–46.
57. Friedrich B, Gronberg H, Landstrom M, Gullberg M, Bergh A. Differentiation stage specific expression of oncoprotein 18 in human and rat prostatic adenocarcinoma. Prostate 1995;27:102–9.
58. Price DK, Ball JR, Bahrani-Mostafavi Z, Vachris JC, Kaufman JS, Naumann RW, Higgins RV, Hall JB. The phosphoprotein Op18/stathmin is differentially expressed in ovarian cancer. Cancer Invest 2000; 18:722–30.
59. Bieche I, Lachkar S, Becette V, Cifuentes-Diaz C, Sobel A, Lidereau R, Curmi PA. Overexpression of the stathmin gene in a subset of human breast cancer. Br J Cancer 1998;78:701–19.